ELSEVIER

Biochimica et Biophysica Acta 1325 (1997) 178–188

BIOCHIMICA ET BIOPHYSICA ACTA
BBA

A voltage- and K^+-dependent K^+ channel from a membrane fraction enriched in contractile vacuole of *Dictyostelium discoideum*

Kunito Yoshida [a,d,*], Toru Ide [a], Kei Inouye [b], Koichi Mizuno [c], Takahisa Taguchi [d], Michiki Kasai [a]

[a] *Department of Biophysical Engineering, Faculty of Engineering Science, Osaka University, Toyonaka 560, Japan*
[b] *Department of Botany, Division of Biological Science, Graduate School of Science, Kyoto University, Kyoto 606-01, Japan*
[c] *Department of Biology, Graduate School of Biological Science, Osaka University, Toyonaka 560, Japan*
[d] *Department of Organic Materials, Osaka National Research Institute, AIST, Ikeda, Osaka 563, Japan*

Received 11 December 1996; accepted 12 December 1996

Abstract

We obtained a membrane fraction enriched in the contractile vacuole by aqueous-polymer two-phase partitioning and its channel activities were analysed by incorporating it into artificial planar lipid bilayers. In asymmetrical KCl solutions (*cis*, 300 mM/100 mM, *trans*), we observed single-channel currents of a highly K^+-selective channel with slope conductance of 102 pS and reversal potential of -20.4 mV, which corresponded to $P_{K+}/P_{Cl-} = 7$. They showed bursts separated by infrequent quiescent periods. At 0 mV the mean open time was 2.0 ms. Among monovalent cations, Na^+ and Li^+ were impermeable, whereas Rb^+ showed permeability equivalent to that of K^+, although the unitary conductance was apparently reduced when the current flowed from the Rb^+ containing side, suggesting that Rb^+ is a permeant blocking ion. The open probability within bursts remained constant at approx.0.6 as long as the holding potential was positive on the *cis* side with respect to the *trans* side, but it decreased to 0 at negative potential. This channel was blocked by submillimolar concentrations of quinine and 30 mM TEA^+. The open probability-voltage relationship showed a striking dependency on the KCl concentration on either side. This channel may play a role in water transport in this organelle.

Keywords: Contractile vacuole; Planar lipid bilayer; Inward rectifier potassium channel; Aqueous-polymer two-phase partitioning; (*D. discoideum*); Quinine

1. Introduction

The contractile vacuole is a prominent structure which can easily be recognized in fresh-water protozoa and amoebae. This organelle is believed to accumulate water from the cytosol and excrete it into the extracellular space, in this way allows fresh-water organisms to survive under hypotonic environments without losing intracellular essential ions. The great

Abbreviations: TEA, tetraethylammonium; EDTA, ethylenediamine-*N*,*N*,*N*′,*N*′-tetraaccetic acid; PMSF, phenylmethylsulfonyl fluoride; NBD-Cl, 7-chloro-4-nitrobenzo-2-oxa-1,3-diazole; Tris, tris(hydroxymethyl)aminomethane; FITC, fluorescein isothiocyanate; Hepes, *N*-2-hydroxyethylpiperazine-*N*′-2-ethanesulfonic acid

* Corresponding author. Fax: +81 6 8506557; E-mail: yoshida@bpe.es.osaka-u.ac.jp

PII S0005-2736(96)00257-X

mystery lies in the mechanism whereby water is pumped up from the more hypertonic cytoplasm and excreted into more hypotonic extraplasmic space. The large amount of water estimated to flow from the cytoplasm into the vacuole suggests the involvement of active transport of salts [1].

Recently, the structure of the contractile vacuole complex in *Dictyostelium discoideum* was investigated in detail by electron microscopy using a quick-freeze, deep-etch technique, which revealed the presence of interconnected array of tubules and cisternae rich in V-H^+-ATPases [2]. This organelle was isolated by sucrose density gradient centrifugation and found to consist of two kinds of vacuoles, the central large vacuole *bladder* and satellite tubules *spongiomes*, as seen in other protozoa [3]. *Spongiomes* are highly enriched in V-H^+-ATPases, which are likely to play an important role in the energetic process of water accumulation. *Bladders* are more buoyant vacuoles which are enriched in alkaline phosphatase activity [3,4] and membrane-bound calmodulin [5], and are believed to be the locus where the contractile vacuole complex fuses with the plasma membrane [6]. *Acidosomes*, which have been isolated from buoyant membrane fractions, are also highly enriched in V-H^+-ATPases [7–9], but its relationship with the contractile vacuole complex remains to be clarified [3,10]. Interestingly, cells of a clathrin heavy chain-deficient mutant lack contractile vacuoles, which implies that a certain mechanism common to clathrin-mediated endocytosis is involved in the generation or retention of this organelle [11].

The mechanisms of water accumulation and extrusion remain controversial. In large amoebae, *Amoeba proteus* and *Chaos chaos*, it has been suggested that the formation of the hypotonic fluid in the vacuole takes place in two steps: First, bulk fluid is brought into the vacuole, by fusion of isotonic vesicles or by passive influx of water following the transport of osmolytes such as K^+ ions. Second, the osmolytes are reabsorbed into the cytoplasm leaving hypotonic fluid behind [1,12,13]. On the other hand, based on the finding that V-H^+-ATPases are present abundantly on the contractile vacuole membranes, Heuser et al. [2] proposed that HCO_3^- is transported into the contractile vacuole by the proton motive force where it acts as an osmolyte causing water to accumulate passively. To understand the mechanism of water-pumping by the contractile vacuole, it is therefore necessary to characterize the ion transport across its membrane. We isolated a membrane fraction enriched in contractile vacuoles by aqueous-polymer two-phase partitioning [14], fused it into artificial planar lipid bilayers, and analysed its channel activities. We focused on a frequently observed channel that was highly K^+-selective and showed unusual voltage-dependency. Part of this work was presented at the 12th International Biophysics Congress, 11–16 August 1996, Amsterdam (Progress in Biophysics and Molecular Biology, 65, suppl. 1, P-C2-07).

2. Materials and methods

2.1. Cells and fractionation by two-phase system

D. discoideum strain AX-2 was cultured in HL-5 medium on a gyratory shaker at 175 rpm, 23°C, to $5 \cdot 10^6 \sim 1 \cdot 10^7$ cells/ml [15]. To obtain starved cells, vegetative cells were washed and shaken in 10 mM Na/K phosphate buffer (pH 6.5) for 5 ~ 9 h at a cell density of $2.0 \cdot 10^7$ cells/ml. Cells were pelleted at $800 \times g$ for 1 min, washed in a homogenate buffer (5 mM glycine/NaOH (pH 8.5), 0.1 M sucrose) [7,8], resuspended in the same buffer supplemented with 1 mM EDTA and protease inhibitors (1 mM PMSF, 1 μg/ml leupeptin), and homogenized by passage through a polycarbonate filter with 5 μm pores. The homogenate was then centrifuged at 1000 $\times g$ for 1 min to remove intact cells and at 122 800 $\times g$ for 1 h, and the resulting pellet was resuspended in 5 mM potassium phosphate buffer (pH 8.0) containing 0.3 M sucrose. About 5 ~ 10 mg protein of the membrane pellet was loaded on aqueous-polymer two-phase system to yield 12-g system in a 15-ml plastic tube with final concentrations of 6.0 ~ 6.4%(w/w) dextran T500, 6.0 ~ 6.4%(w/w) poly(ethylene glycol) (PEG 4000), 3 mM KCl, 0.3 M sucrose, and 5 mM potassium phosphate (pH 8.0). Each tube was prepared by weighing contents separately. Membranes were partitioned three times and re-extraction was performed as described in Ref. [14]. The upper poly(ethylene glycol) phases and the first partitioned lower phase, were separately collected and diluted 5–10-fold with a buffer consisting of 10 mM Tris and 20 mM Hepes (pH 7.4). After cen-

trifuged at $122\,800 \times g$ for 1 h, the resulting pellet was resuspended in the same buffer containing 0.3 M sucrose. The final protein concentration was $2 \sim 5$ mg/ml. The samples were stored in $30 \sim 50$ μl aliquots at -70°C until use.

2.2. Marker enzyme assays

Protein was determined with BioRad Protein Assay kit using bovine serum albumin as a standard [16]. Alkaline phosphatase and NADH oxidoreductase were assayed as described in Ref. [17], acid phosphatase as described in Ref. [8], and ATPase as described in Ref. [7]. NBD-Cl-sensitive ATPase activity was determined as the difference between the activities in the presence and absence of 25 μM NBD-Cl. Vanadate-sensitive ATPase activity was determined as the difference between the activities in the presence and absence of 100 μM vanadate. Mitochondrial ATPase activity was measured at pH 9.5.

2.3. FITC-labelling of cell surface

Cells were washed in 5 mM $NaHCO_3$/NaOH (pH 9.5), 0.1 M sucrose, and resuspended in the same solution containing 400 μg/ml FITC at a cell density of approx. $5 \cdot 10^8$ cells/ml [18]. After shaken at 23°C for 5 min, cell suspension was diluted at least

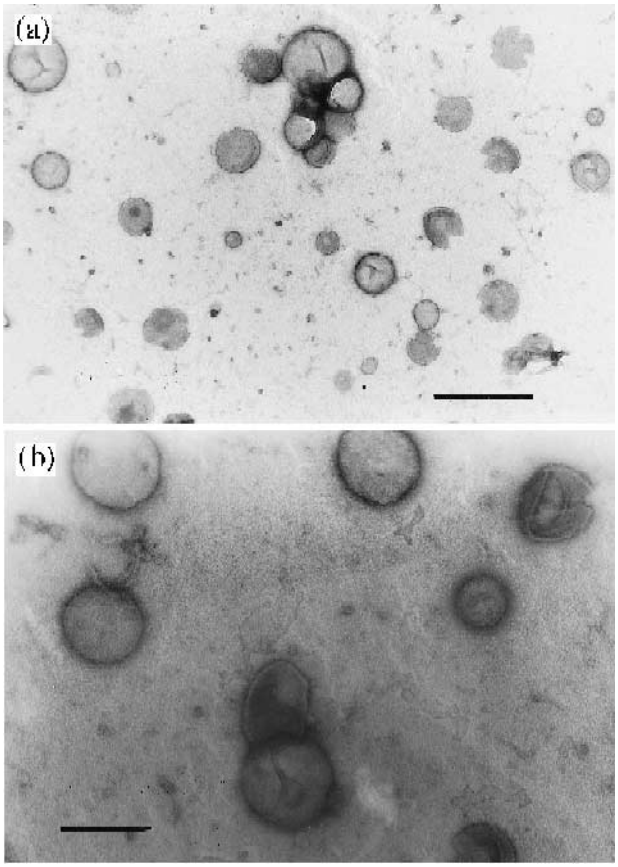

Fig. 1. Negatively-stained electron micrographs of a sample from the upper phase. Bar = (a) 500 nm, (b) 200 nm.

Table 1
Characteristics of the crude membrane pellet and the partitioned fraction

Marker	Activity in crude membrane (nmol/min)	Activities in two phase fractions (% of crude membrane)		Enrichments
		Upper	Lower	
Protein	16.6 (mg)	7.5	44.7	–
Alkaline phosphatase [a]	104	37.7	34.4	4.9
NBD-Cl-sensitive ATPase [b]	4500	3.2	102.2	0.44
Vanadate-sensitive ATPase [c]	2940	6.0	67.7	0.78
Cell-surface label	–	2.9	53.4	–
Acid phosphatase [d]	5190	1.4	45.3	0.21
NADH oxidoreductase [e]	16200	1.0	72.7	0.13
Mitochondrial ATPase	12300	2.9	50.4	0.39

Membrane was pelleted from the homogenate of 5 ~ 7-h developed cells ($\sim 2 \cdot 10^9$ cells) and subsequently partitioned by a two-phase system composed of 6.0% dextran-6.0% poly(ethylene glycol). Averages of three samples (one of which is FITC-labelled) are shown except for cell-surface label, where means of two independent experiments are shown. Enrichments were calculated as the specific activities (nmol/min per mg) of the upper fraction divided by those of the crude membrane

[a] A marker for contractile vacuole; [b] a marker for *acidosome*; [c] a marker for plasma membrane; [d] a marker for endosome/lysosome; [e] a marker for endoplasmic reticulum.

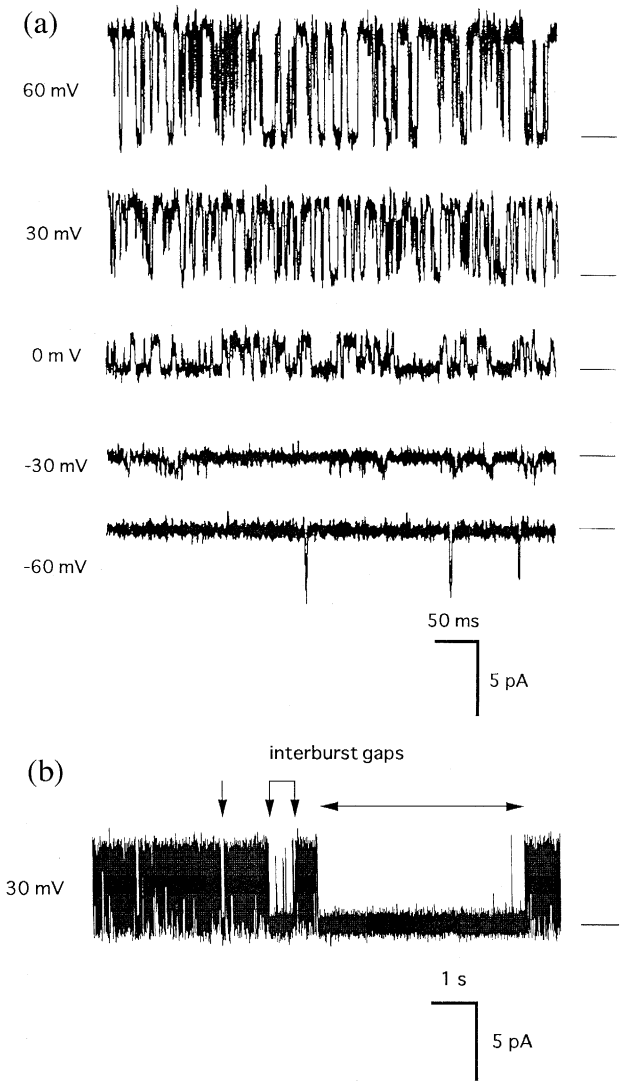

Fig. 2. (a) Single-channel recordings of the *Dictyostelium* K^+ channel. Applied voltages are indicated at the left of each trace. The lines on the right-hand side show the baseline current. The bathing solution consisted of (*cis*/*trans*) 300:100 mM KCl, 10 mM Tris, 20 mM Hepes (pH 7.4). (b) A single-channel recording in a more compressed scale to show long silent periods. Conditions are the same as in (a).

30-fold in ice-cold 5 mM glycine/NaOH (pH 9.5), containing 0.1 M sucrose. Cells were centrifuged and the pelleted cells were resuspended and washed three times in 5 mM glycine/NaOH (pH 8.5), containing 0.1 M sucrose. Little cell lysis was observed under these conditions. The specificity of cell surface labelling was evaluated by fluorescence quenching upon acidification of the solution to pH 4 by addition of

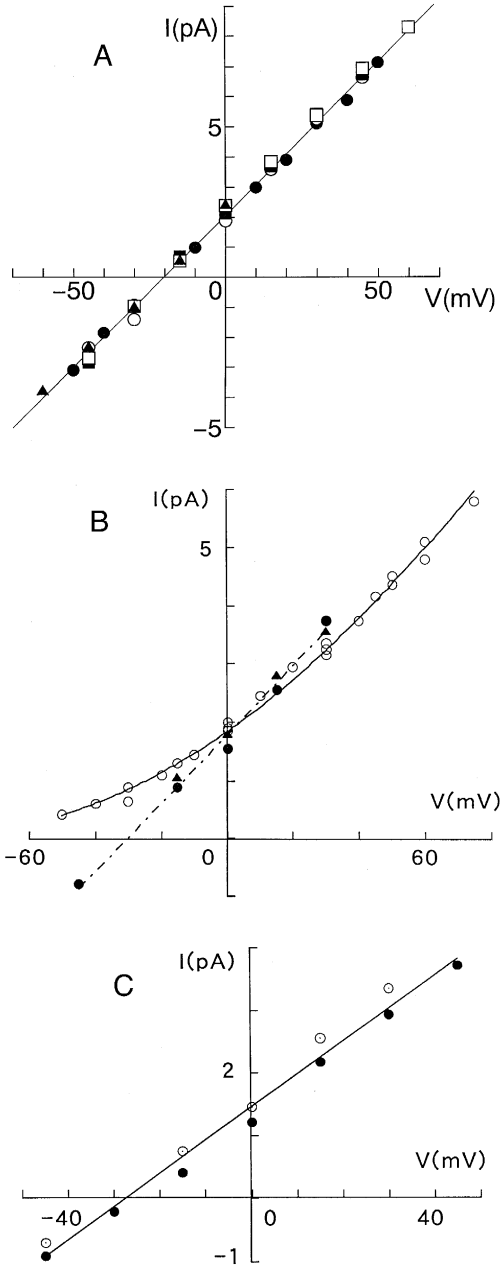

Fig. 3. Current-voltage relationships of the *Dictyostelium* K^+ channel obtained in different salt solutions. The composition of the solutions (*cis*/*trans*) are, (A) 300 mM KCl:100 mM KCl, (B) 100 mM KCl:100 mM NaCl (open circles), 100 mM KCl:80 mM NaCl + 20 mM KCl (closed symbols), (C) 100 mM KCl:80 mM LiCl + 20 mM KCl, each buffered with 10 mM Tris, 20 mM Hepes (pH 7.4). Data from independent (A) 5, (B) 2 (closed symbols), (C) 2 bilayers are represented by different symbols. The lines shown here were generated by regression with combination of all the data from different bilayers with the same solution. For (B) (open circles), the curve was generated according to the GHK equation assuming that Cl^- is impermeable.

HCl. About 90% of the fluorescence was quenched upon acidification in these experiments described, whereas a considerable amount of fluorescence was resistant to acidification if pH below 9.5 was used. Aliquots of membrane fractions obtained by the two-phase method were suspended in buffer containing 1 mM Tris, 2 mM Hepes, 0.1 M sucrose, and 0.1% Triton X-100 (pH 7.4), and fluorescence was measured at excitation and emission wave lengths of 495 and 520 nm, using a spectrophotometer. Basal fluorescence of cell lysates without FITC has been subtracted from all measurements.

2.4. Electrophysiology

Planar lipid bilayers were prepared with soybean L-α-phosphatidylcholine dissolved at 20 mg/ml in n-decane [19]. Prepared samples were mixed with a half volume of 3 M KCl (to yield a final concentration of 1 M KCl) and fused into the bilayer by pressure application. The recording solutions were composed of the indicated concentrations of salts and 10 mM Tris, 20 mM Hepes (pH 7.4). A 50-GΩ resistive-feedback current-to-voltage converter was built according to [20]. Signals were recorded on videotapes after processing with a digital audio processor (PCM-501ES; SONY Corp.).

2.5. Data analysis

Electrical signals were regenerated from the stored videotapes, filtered at 1 kHz, digitized at 5 kHz, and

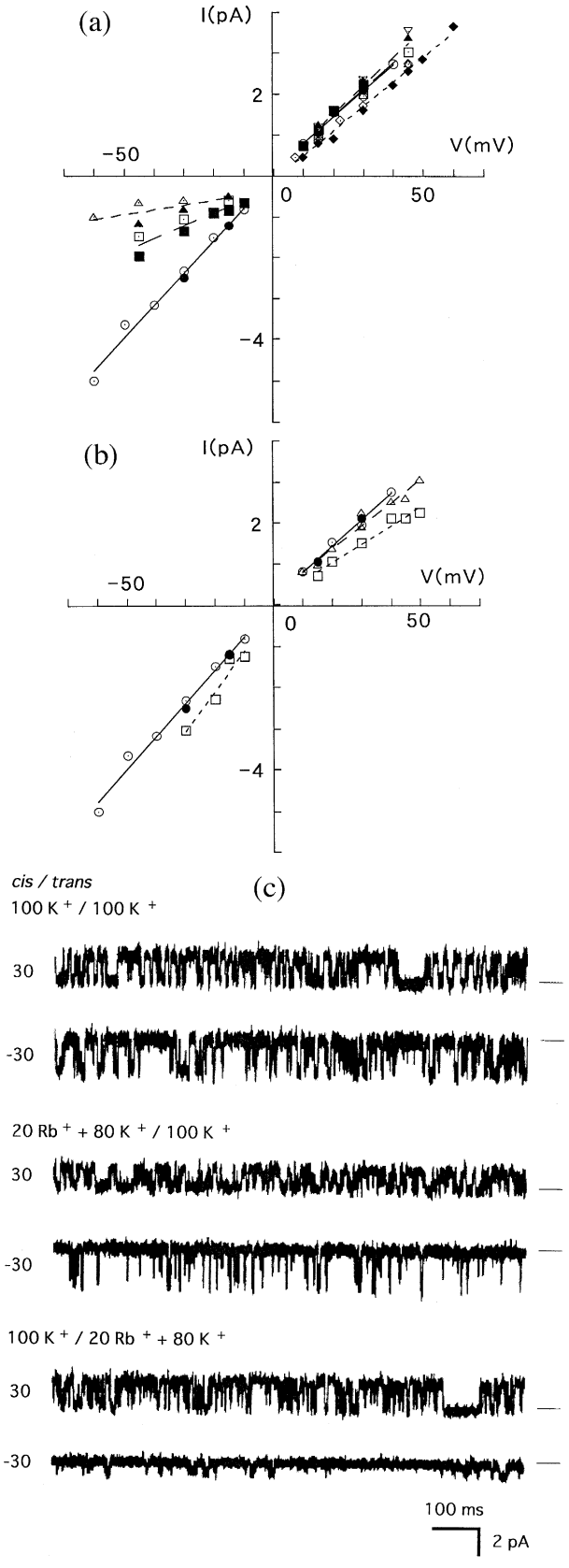

Fig. 4. Current-voltage relationships of the *Dictyostelium* K^+ channel in the presence of Rb^+. Data from independent 2 bilayers (filled and open symbols) are shown. (a) Effects of Rb^+ present on the *trans* side. *Cis* side = 100 mM KCl, *trans* side = 100 mM KCl (circles), 10 mM RbCl + 90 mM KCl (squares), 20 mM RbCl + 80 mM KCl (triangles), 80 mM RbCl + 20 mM KCl (diamonds). (b) Effects of Rb^+ present on the *cis* side. *Cis* side = 100 mM KCl (circles), 10 mM RbCl + 90 mM KCl (triangles), 20 mM RbCl + 80 mM KCl (squares), with *trans* side = 100 mM KCl. All the solutions were buffered with 10 mM Tris, 20 mM Hepes (pH 7.4). The lines shown here were generated by regression with combination of all the data from different bilayers with the same solution. (c) The corresponding channel traces. From top to bottom: (*cis* 100 mM KCl/*trans* 100 mM KCl) 30 mV, −30 mV, (*cis* 20 mM RbCl + 80 mM KCl/*trans* 100 mM KCl) 30 mV, −30 mV, (*cis* 100 mM KCl/*trans* 20 mM RbCl + 80 mM KCl) 30 mV, −30 mV.

analyzed by pCLAMP software (Axon Instrument). In this paper, voltages of the *cis* (sample-applying) side relative to the *trans* side are shown, and the sign of the current is positive when it flows from *cis* to *trans*.

For the statistical curve-fitting, the lines and curves were generated by the least-square fitting method using computer softwares (KaleidaGraph 3.0 for Macintosh or Ngraph v.5.31 for NEC PC-9801).

2.6. Materials

Dextran T500 was purchased from Pharmacia, PEG 4000 from Kishida Kagaku (Osaka, Japan), FITC from Dojindo Laboratories (Kumamoto, Japan), L-α-phosphatidylcholine, quinine, cAMP, cGMP from Sigma, folic acid from Wako (Osaka, Japan) and charybdotoxin from Peptide Institute (Osaka, Japan).

3. Results

3.1. Characterization of the sample preparation

A high-speed precipitate of a cell homogenate was fractionated into two phases by a poly(ethylene glycol)-dextran system as described in Section 2. As shown in Table 1, markers of the plasma membrane, 'acidosome', endosomes/lysosomes, endoplasmic reticulum, and mitochondria were predominantly partitioned in the lower phase, whereas alkaline phosphatase, a marker for contractile vacuoles in *Dictyostelium* [3,4], but see Ref. [21] was enriched 5-fold in the upper phase. We concluded that our phase system preferentially extracts contractile vacuoles from cell homogenates.

Fig. 1 shows electron micrographs of negatively stained vesicles from the upper phase. These vesicles show the characteristics of contractile vacuoles previously described, such as large angular holes and smooth and crispy membrane surfaces [3].

3.2. Frequency of observing channel activities

When these preparations were incorporated into a lipid bilayer, we observed many kinds of conductive activities. Most of these activities showed very fast or irregular gating kinetics. In this paper, we concentrated on a specific channel with reproducible characteristics which appeared in 59 bilayers of a total of 2290 trials. This channel showed a strong voltage-dependency such that it opened at a high probability when the *cis* side (sample-applying side) was positive while it closed when the *cis* side was negative (Fig. 2a). In another 9 bilayers, the same channel was

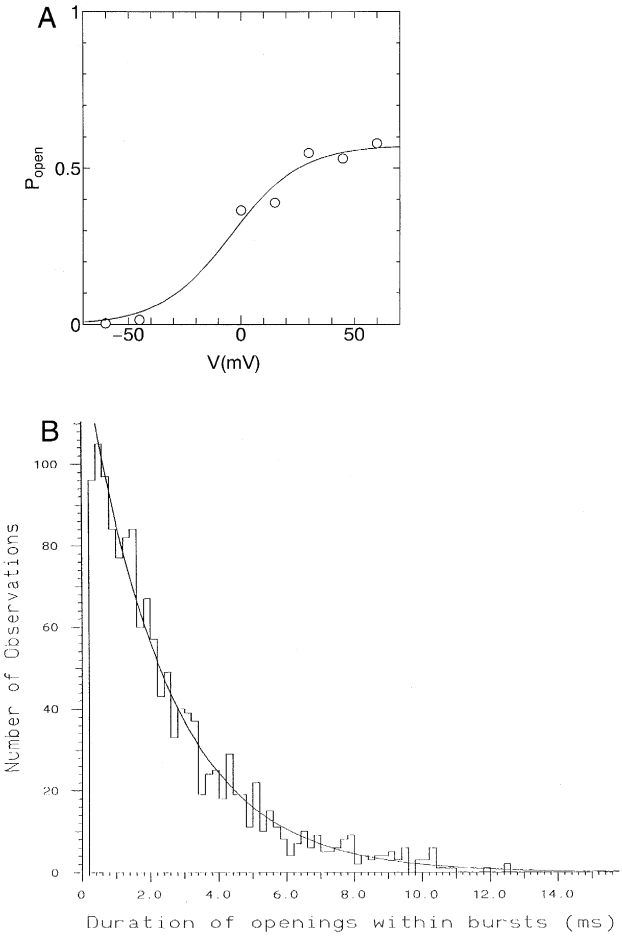

Fig. 5. Open probability (A) and open time distribution (B) in the burst period. The analyses were performed on the recordings shown in Fig. 2a. In (A), data are fitted according to Boltzmann's equation $P_{open} = 1/[1/P_{open}^{max} + \exp\ \{ze(V_0 - V)/kT\}]$ where P_{open}^{max} is maximal open probability, z an equivalent valence, e the elementary charge, V_0 the voltage of half-maximal activation, V voltage, k the Boltzmann's constant, and T temperature. For this case, $P_{open}^{max} = 0.57$, $z = 1.6$, and $V_0 = 4.34$ mV was obtained. In (B), the histogram shows the number of openings per bin of 0.2 msec width. The continuous line shows an exponential probability density function that has been fitted to the observations (above 0.4 ms) by the maximum likelihood method. It has a time constant of $\tau = 2.0$ ms at $V = 0$ mV.

observed in reverse orientation. Since the sidedness of the vesicle membrane of the preparations is unknown, the orientation of the channel within the cell remains to be determined.

3.3. Conductance size and ion selectivity

Representative traces of single channel currents recorded in asymmetrical (*cis / trans*) 300:100 mM KCl solutions are shown in Fig. 2. The current-voltage (*I-V*) relationship revealed a slope conductance of 102.3 ± 2.8 pS and a reversal potential of -20.4 ± 0.8 mV which corresponds to $P_K + / P_{Cl} - = 7$ (Fig. 3A, $n = 5$). In asymmetrical (*cis / trans*) 100 mM KCl:100 mM NaCl solutions, the slope conductance was 57.1 pS at positive holding potentials but the *I-V* relationship shows non-linearity at negative potentials and the *I-V* curve never intersects the V-axis (Fig. 3B, open circles). In asymmetrical solutions which contains 100 mM KCl in the *cis* side and 80 mM NaCl plus 20 mM KCl in the *trans* side, the relationship was almost linear between -45 and 30 mV, the slope conductance and the reversal potential being $57.9 \sim 1.2$ pS and -31.5 ± 1.7 mV, respectively (Fig. 3B, closed symbols, $n = 2$). The permeability ratio P_{Na+}/P_{K+} was calculated to be almost 0 according to the Goldman–Hodgkin–Katz equation, that is, Na^+ is an impermeable ion. Similarly, Li^+ was shown to be impermeable (Fig. 3C).

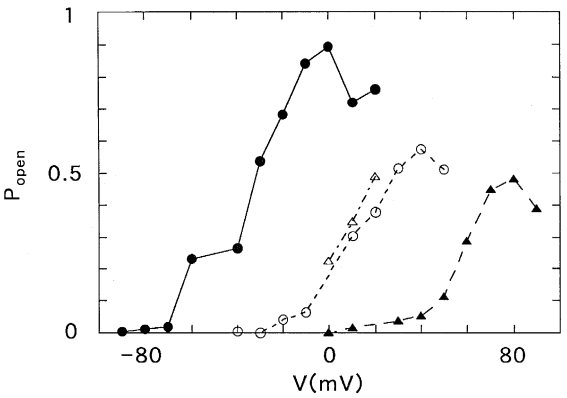

Fig. 6. Voltage-dependence of open probabilities shifted by changes in the *trans* concentration of K^+ ion. In one experiment, the *trans* side solution was sequentially exchanged by perfusion from 30 mM (closed circles), to 300 mM (open circles), to 1000 mM (closed triangles), and finally to 100 mM (open triangles) KCl. *Cis* side solution was 300 mM KCl for all records. The values of half-activation voltage were approximately -30 mV in 30 mM *trans* KCl, 10 mV in 300 mM KCl, and 60 mV in 1000 mM KCl, respectively, whereas the values of reversal potential were -50.6 mV, 1.2 mV, and 26.6 mV, respectively (not shown).

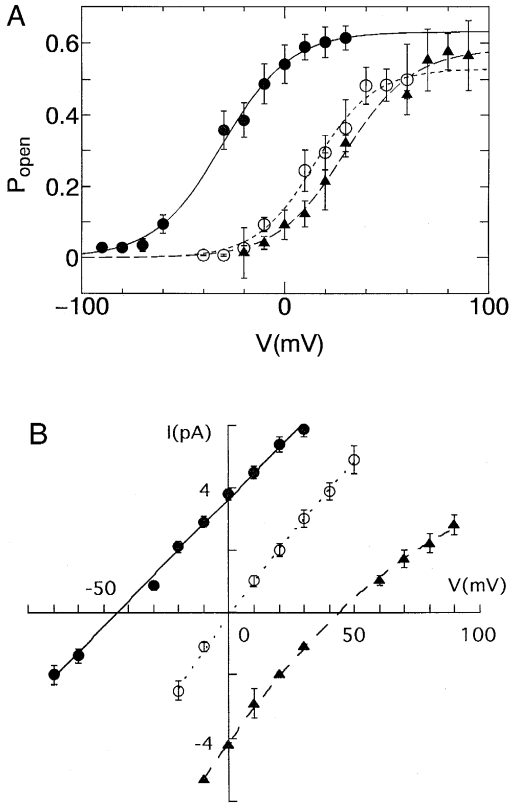

Fig. 7. (A) Voltage-dependence of open probabilities in various concentrations of K^+ ion. (B) The corresponding current-voltage relationship. The means $\pm$ S.E. are shown. *Cis / trans* solution was 300:30 mM (closed circles, $n = 8$), 300:300 mM (open circles, $n = 5$), and 30:300 mM (closed triangles, $n = 3$) KCl. In (A), the data are fitted according to the Boltzman equations in the same way as in Fig. 5A. The values of P_{open}^{max} are 0.63, 0.53, and 0.58, respectively. The values of z are 1.5, 1.7, and 1.5, respectively. The values of V_0 are -23.3, 24.1, and 38.3 mV, respectively. In (B), the data are fitted according to quadratic equations. The values of the reversal potential were, -43.6, -0.8, and 43.9 mV, respectively.

On the other hand, the behaviour of Rb^+ was more complex. When part of K^+ ions on the *trans* side in symmetrical KCl solutions was replaced by Rb^+ ions, the observed currents at negative holding potentials (i.e., potentials driving the Rb^+ ions across the channel) were reduced (Fig. 4a). Rb^+ ions present in the *cis* side solution, on the contrary, did not affect the currents irrespective of the direction of the holding potential (Fig. 4b). The corresponding traces are

shown in Fig. 4c. The reversal potential obtained by interpolation was approx. 0 mV with all Rb^+/K^+ ratio examined, indicating that the permeability ratio P_{Rb+}/P_{K+} was approximately 1. These results pointed out that Rb^+ ion is permeant but it blocks this channel effectively at the same time.

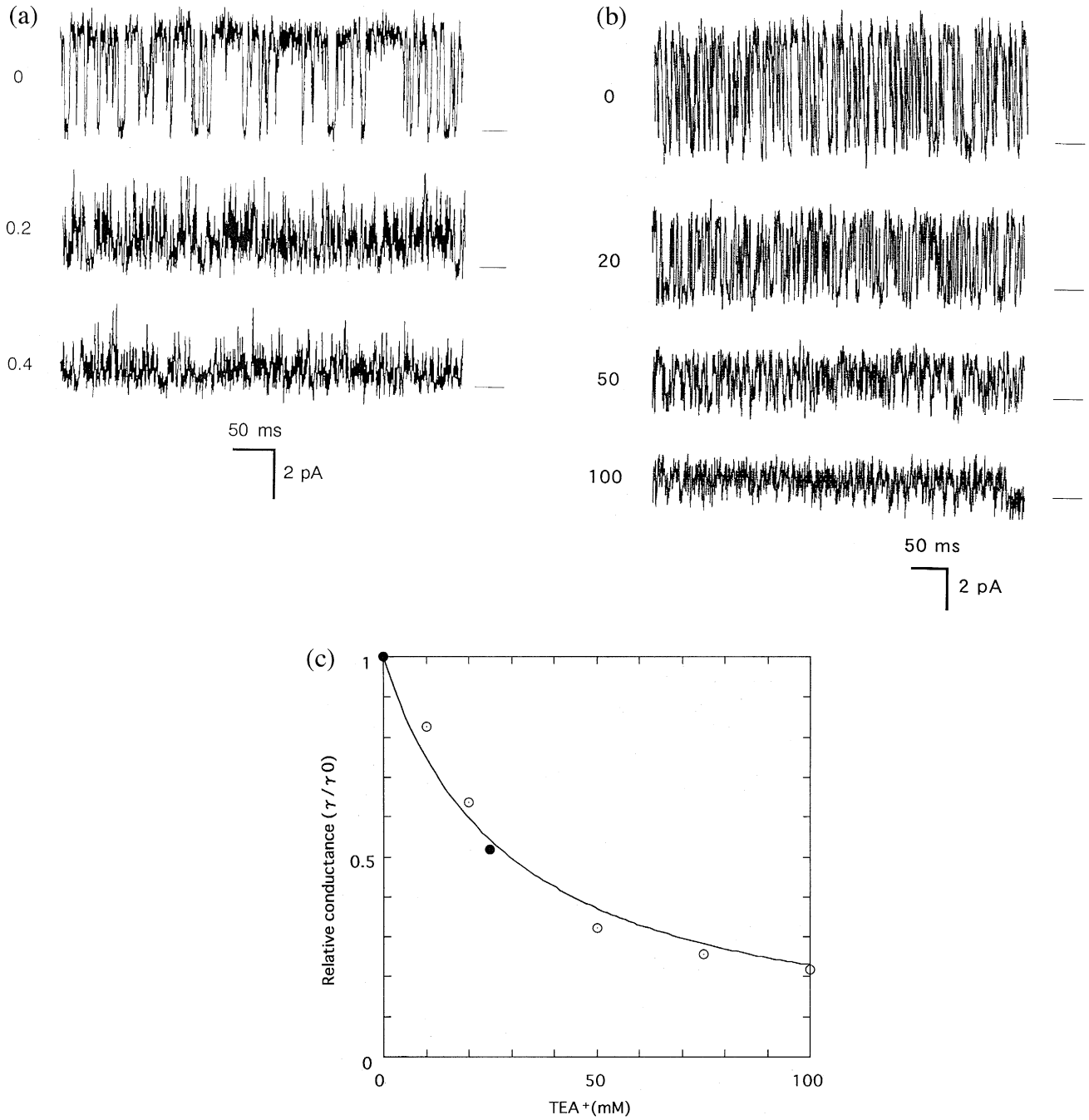

Fig. 8. Blockade of the *Dictyostelium* K^+ channel by quinine (a) and TEA^+ (b), applied from the *cis* side. In (a) and (b), the concentrations of the drugs are shown to the left. *Cis/trans* solution was 300:100 mM KCl. Holding potential = 30 mV. (c) Dose-effect relationship of TEA^+ blockade. The curve shown is the best fit of the data from 2 independent bilayers (represented by different symbols), assuming the following equation, $\gamma/\gamma_0 = 1/(1 + [TEA^+]/K_d)$, where γ denotes the conductance at the indicated TEA^+ concentrations and γ_0 without TEA^+, and $K_d = 30$ mM.

3.4. Gating properties

The open probability of this channel was dependent on the applied potential, becoming almost 0 at negative potentials (Fig. 5a). As seen in Fig. 2b, long silent periods were frequently observed, especially at positive potentials. We analyzed open probabilities only within bursts, ignoring closed events longer than 100 ms at positive potentials. Open probability appeared to saturate at approx. 0.6. As shown in Fig. 5b, the open time histogram fitted well to a single-exponential curve of $\tau = 2.0$ ms at 0 mV.

The *trans* side of a bilayer was perfused successively with solutions of varied KCl concentrations (while the *cis* side was held constant at 300 mM KCl). The open probability curve shifted dramatically to the positive direction when the KCl concentration was raised (Fig. 6). The maximal open probability was also lowered when the *trans* KCl concentration was raised from 30 to 300 mM and from 300 to 1000 mM. This decrease in the open probability was recovered after lowering the KCl concentration to 100 mM.

Fig. 7A shows the open probabilities of the channels in *cis* 300 mM; *trans* 30 mM, *cis* 300 mM; *trans* 300 mM, and *cis* 30 mM; *trans* 300 mM KCl solutions plotted against the applied voltage. The voltages of half-maximal activation, estimated by curve-fitting (see Section 4), were −23.3 mV, 24.1 mV, and 38.3 mV, respectively. The reversal potentials were obtained from the corresponding I-V curves (Fig. 7B) to be −44.2 mV, 1.8 mV, and 48.1 mV, respectively. It is obvious that the *trans* K^+ concentration greatly affects the open-probability-voltage relationship, whereas the *cis* K^+ concentration affects only slightly. The maximal open probabilities, estimated by curve-fitting, were 0.63, 0.53, and 0.58, respectively.

3.5. Blockers

Effects of well known K^+ channel blockers, quinine, tetraethylammonium (TEA^+), and charybdotoxin were examined. Quinine blocked this channel effectively at submillimolar concentrations (Fig. 8a). TEA^+ blocked this channel at relatively high concentration, i.e., with K_d of about 30 mM (Fig. 8b,c). Apparent conductance size was reduced when the concentration of TEA^+ was raised. In addition, TEA^+ seemed to increase the open duration, which strongly suggests that this is due to open-channel block. In both cases, the block was reversible (not shown). Charybdotoxin, up to 300 nM, did not block this channel.

3.6. Effects of second messengers

We tested 1 mM cyclic AMP, 10 μM cyclic GMP, 2 mM ATP, and 1 μM folic acid on this channel for their effects on this channel. We did not observe any obvious effects of these agents applied on either side of this channel.

We investigated whether this channel shows Ca^{2+}-dependency using Ca^{2+}-EGTA buffer, but could not find any major effects on its gating activities.

4. Discussion

Aqueous-polymer two-phase partitioning is an established method for isolation of right-side-out vesicles of plasma membrane [14]. We found that membrane preparations obtained from *Dictyostelium* cells by this method were poor in the plasma membrane markers, such as vanadate-sensitive ATPase and cell-surface labels, but instead highly enriched in alkaline phosphatase activity. In *Dictyostelium*, it has been clearly shown by electron-microscopic cytochemistry that this enzyme is localized in contractile vacuoles [3,4]. Additionally, the negatively stained images of our preparations were morphologically indistinguishable from those of the purified contractile vacuoles, characterized by large holes, and smooth and crispy membrane surface. We concluded that the upper phase of the two-phase is rich in contractile vacuoles under our experimental conditions.

By incorporating these contractile vacuole-enriched fraction into planar lipid bilayer, we observed single K^+ channel currents as described above. We are inclined to think that this channel resides on the contractile vacuole membranes. In support of this, we have fairly often encountered similar channel activities in buoyant subcellular fractions obtained by successive centrifugation in 45% and 12% sucrose solutions, which contain contractile vacuoles (Yoshida, K., unpublished observations. Also see Refs. [8,9]).

However we cannot rule out at the moment the possibility that this channel derived from other membranes, because we observed this channel in only 3.0% of the total trials (Section 3.1), which is comparable to the percentage of the contaminated membranes recovered in the samples. We did not investigate whether the lower-partitioned fraction contain the same K^+ channel activity because it often exhibited unidentified conductive activities, which destabilized the planar bilayer and made the measurements almost impossible. Since the contractile vacuole regularly fuses to the plasma membranes, it is well possible that the same channel exists on both membranes.

Two types of K^+ channels (DI and DII) have been described in the plasma membrane of aggregative cells of *Dictyostelium* by cell-attached patch-clamp [22]. However, they are most likely different from ours because DI showed voltage-independent mean open-time of 21 ms within a burst, which is distinct from our channel which shows voltage-dependent mean-open time around 2.6 ms. As for DII, available information is limited, but the overall pattern of the traces is clearly different from that of our channel.

Our channel was almost completely impermeable to Na^+ and Li^+ ions, but permeable to Rb^+ ions. However, the conductance was apparently reduced when the current flowed from the Rb^+ containing side to the other. Such a behaviour of Rb^+ as a permeable blocker was also reported for other K^+ channels [23]. The conductance of this channel saturates at approx. 100 pS (Fig. 3A, Fig. 7B), a large conductance comparable to that of the maxi Ca^{2+}-activated K^+ (BK) channel. However, Ca^{2+} did not have any obvious effects on the gating of this channel, and charybdotoxin, a blocker of BK channel, did not block this channel. It is noteworthy that the conductance also depends on the K^+ concentration of the side into which K^+ ions flow.

When the KCl concentration on either side was varied, the open probability-voltage relationships was shifted to the same direction as the changes in the equilibrium potential of potassium ions (E_K). Such voltage-dependent gating with regard to E_K is a well-known property of the inward rectifier K^+ channels. In our channel, the KCl concentration on the *trans* side greatly affected the half-maximal activation voltage (V_o; see Fig. 5 legend), whereas the KCl concentration on the *cis* side showed much weaker effects. It has been shown that rectification of the inward rectifier K^+ channel in starfish egg depends only on the membrane potential (E) but not on the K^+ equilibrium potential (E_K) when E_K is altered by changing the internal K^+ concentration at a fixed external K^+ concentration, while it depends on $E - E_K$ when E_K is altered by changing the external K^+ at a fixed internal K^+ concentration [24]. As for inward rectifiers, voltage-dependent block by intracellular cations such as Mg^{2+} ions or polyamines is considered to be the cause for the rectification. As for our channel, blockade by such extrinsic cations is unlikely, because divalent cations had been removed by EDTA during sample preparations and no such cations were added (except $Tris^+$). In the ClC-0 voltage-dependent chloride channel, binding of permeant anions to sites in the pore is necessary to open the intrinsic gate [25]. By analogy to the inward rectifiers and ClC-0, voltage-dependent binding of K^+ ions to sites on the *trans* side surface or in the pore may lead to closure of the intrinsic gate or blockade by K^+ ion itself. Blockade of this channel by another permeant ion Rb^+ is intriguing, but further study is necessary to identify the binding sites for these cations.

The physiological roles of this channel in the function of the contractile vacuole remain to be clarified. We recently found that inclusion of quinine in a hypotonic medium caused abnormal swelling of contractile vacuoles and rounding-up of the cell shape, suggesting that some quinine-related activities may be involved in the function of contractile vacuole (Yoshida et al., manuscript in preparation). Quinine at a concentration range which blocked our channel was previously shown to exert various effects on the physiology of *Dictyostelium* cells, i.e., inhibition of cyclic AMP-induced K^+ release [26,27], inhibition of cyclic AMP-induced hyperpolarization [28], and formation of long-stalked fruiting bodies [29]. These phenomena were interpreted as consequences of the effects of quinine on a hypothetical plasma membrane K^+ channel. However they may be equally attributable to the effects of blockade by quinine of the contractile vacuole channel observed in this study since quinine is membrane-permeant.

The membrane potential of contractile vacuole in *Amoeba proteus* is 10 to 20 mV positive luminal side to cytoplasmic side [30]. The presence of an inside-

positive membrane potential in the contractile vacuole suggests that voltage-dependent channels may exist in that membrane. Our channel may be one such channel whose function, for example, is to reabsorb K^+ ion from inside the contractile vacuole to the cytosol before the vacuole discharges its content. The rectifying property of this channel would then prevent the opposite flow of the K^+ ions. Identification of the gene would help to clarify its functions.

Acknowledgements

We are especially grateful to Shigetoshi Oiki and Bert Van Duijn for reading the manuscript and giving us many helpful suggestions, to John Heuser for earlier encouragements, to Koji Okamoto, Mineko Maeda, Atsuko Iwane, Yohko Yamada, and Hiroaki Tabuchi for facilities of culture and experiments, to Tadanao Ando for opportunities to use a polarimeter, to Yoshiro Tatsu for suggestions on fluorescence labelling, to Manabu Tanifuji for technical advice on perfusion, to Kazuyuki Kiyosue, Hiroto Sakamoto, Naohiro Yamaguchi, and Hiroko Yoshida for practical help and suggestions. K.Y. is a fellow of NEDO.

References

[1] Zeuthen, T. (1992) Biochim. Biophys. Acta 1113, 229–258.
[2] Heuser, J., Zhu, Q. and Clarke, M. (1993) J. Cell. Biol. 121, 6, 1311–1327.
[3] Nolta, K.V. and Steck, T.L. (1994) J. Biol. Chem. 269, 3, 2225–2233.
[4] Quiviger, B., De Chastellier, C. and Ryter, A. (1978) J. Ultrastruct. Res. 62, 228–236.
[5] Zhu, Q. and Clarke, M. (1992) J. Cell. Biol. 118, 2, 347–358.
[6] De Chastellier, C., Quiviger, B. and Ryter, A. (1978) J. Ultrastruct. Res. 62, 220–227.
[7] Padh, H., Lavasa, M. and Steck, T.L. (1989) J. Cell Biol. 108, 865–874.
[8] Padh, H., Lavasa, M. and Steck, T.L. (1989) Biochim. Biophys. Acta 982, 271–278.
[9] Nolta, K.V., Padh, H. and Steck, T.L. (1991) J. Biol. Chem. 266, 27, 18318–18323.
[10] Padh, H. and Tanjore, S. (1995) FEBS Lett. 368, 358–362.
[11] O'Halloran, T.J. and Anderson, R.G.W. (1992) J. Cell Biol. 118, 6, 1371–1377.
[12] Schmidt-Nielsen, B. and Schrauger, C.R. (1963) Science 139, 606–607.
[13] Riddick, D., H. (1968) Am. J. Physiol. 215, 736–740.
[14] Larsson, C., Widell, S. and Kjellbom, P. (1987) Methods Enzymol. 148, 558–568.
[15] Sussman, M. (1987) Methods Cell Biol. 28, 9–29.
[16] Bradford, M.M. (1976) Anal. Biochem. 72, 248–254.
[17] Siu, C.H. and Lerner, R.A. (1977) J. Mol. Biol. 116, 469–488.
[18] Edidin, M. (1989) Methods Cell Biol. 29, 87–102.
[19] Mueller, P. and Rudin, D.O. (1969) in Laboratory Techniques in Membrane Biophysics (Passow, H. and Stepfli, R. eds.), pp. 141–156, Springer, Berlin.
[20] Sigworth, F.J. (1983) in Single-channel Recording (Sakmann, B. and Neher, E., eds.), pp. 3–35, Plenum, New York.
[21] Glomp, I., Schäfer, D. and Hess, B. (1985) Histochemistry 83, 251–255.
[22] Müller, U. and Hartung, K. (1990) Biochim. Biophys. Acta 1026, 204–212.
[23] Silver, M.R., Shapiro, M.S. and DeCoursey, T.E. (1994) J. Gen. Physiol.103, 519–548.
[24] Hagiwara, S. and Yoshii, M. (1979) J. Physiol. 292, 251–265.
[25] Pusch, M., Ludewig W., Rehfeld, A. and Jentsch, T.J. (1995) Nature 373, 527–531.
[26] Aeckerle, S., Wurster, B. and Malchow, D. (1985) EMBO J. 4, 39–43.
[27] Aeckerle, S. and Malchow, D. (1989) Biochim. Biophys. Acta 1012, 196–200.
[28] Van Duijn, B. and Wang, M. (1990) FEBS Lett. 275, 201–204.
[29] Van Duijn, B., Van der Molen, L.G. and Ypey, D.L. (1989) Pflugers Arch. 414 (Suppl. 1), S148–S149.
[30] Prusch, R.D. and Dunham, P.B. (1967) J. Gen. Physiol. 50, 1083.